Molecular Association in Nematic Phases of Cyclic Liquid Crystal Oligomers

V. V. Tsukruk,*,† T. J. Bunning,‡ H. Korner,§ C. K. Ober,§ and W. W. Adams||

College of Engineering and Applied Sciences, Western Michigan University, Kalamazoo, Michigan 49008, Science Application International Corporation, 101 Woodman Drive, Suite 103, Dayton, Ohio 45431, Department of Materials Science and Engineering, Cornell University, Ithaca, New York 14853, Wright Laboratory/MLPJ, Building 651, 3005 P Street, Ste 1, Wright-Patterson Air Force Base, Ohio 45433-7702

Received May 29, 1996; Revised Manuscript Received September 11, 1996⊗

ABSTRACT: We analyzed molecular ordering in the nematic phase of cyclic LC oligomers with mesogenic groups attached to a central siloxane ring. We focus on relationships between the local spatial arrangement of these molecules and low-angle X-ray scattering phenomena as revealed by computer molecular modeling. Computer simulation shows that the presence of strong low-angle X-ray reflections in the nematic phase is caused by local association of the molecules. The cyclic molecules form double-row associations with up to six molecules packed in a single string. The presence of the siloxane central rings with a high local concentration of Si−O atomic groups with strong scattering power is critical for the appearance of these low-angle X-ray reflections with significant intensity. Cycling of siloxane groups into short rings hinders rotation and restricts mobility of these fragments, resulting in a high localization of strong scattering groups. Computer simulation of X-ray properties of partially ordered systems within the "lattice approximation" works well for crystal lattices and highly ordered mesophases like smectics. However, this approach underestimates local distortions of positional ordering and does not adequately describe short-range molecular ordering in the nematic phase. Application of straightforward calculations of the form-factor of molecular clusters reproduces major features of these unusual X-ray scattering patterns but falls short in describing fine details such as diffuse background scattering, peak profiles, and exact *d*-spacings.

Introduction

The classical model of molecular organization within a nematic phase of low molar mass liquid crystals (LCs) assumes uniform orientational ordering of the anisotropic molecules along a unique direction and unrestricted freedom of transversal and longitudinal displacements of molecules (Figure 1).[1] Usually, short-range positional molecular ordering is expanded over three to four coordinate spheres. Various more complicated versions of nematic ordering with local molecular associations have been observed in nematic phases of various LCs and polymeric LCs with stronger intermolecular interactions.[2−14] The most known case is cybotactic nematics, where association of molecules in small clusters or "cybotactic" groups occurs (Figure 1b).[2] Another type of association observed previously in a few systems is shown in Figure 1c. Molecular association of the mesogens in a single row along the director is termed "string" formation.[5] The local positional correlations of anisotropic molecules in these nonclassical nematic phases are considered to be responsible for atypical low-angle X-ray scattering (strong diffuse meridional reflections) observed for oriented mesophases.

A class of "hybrid" LC compounds, wherein a small cyclic backbone is modified by pendant mesogenic units, has shown a strong tendency to show periodic diffuse meridional reflections, as shown shematically in Figure 1c.[4] Properties of these oligomeric LC compounds with several (typically four to six) chemically linked mesogens

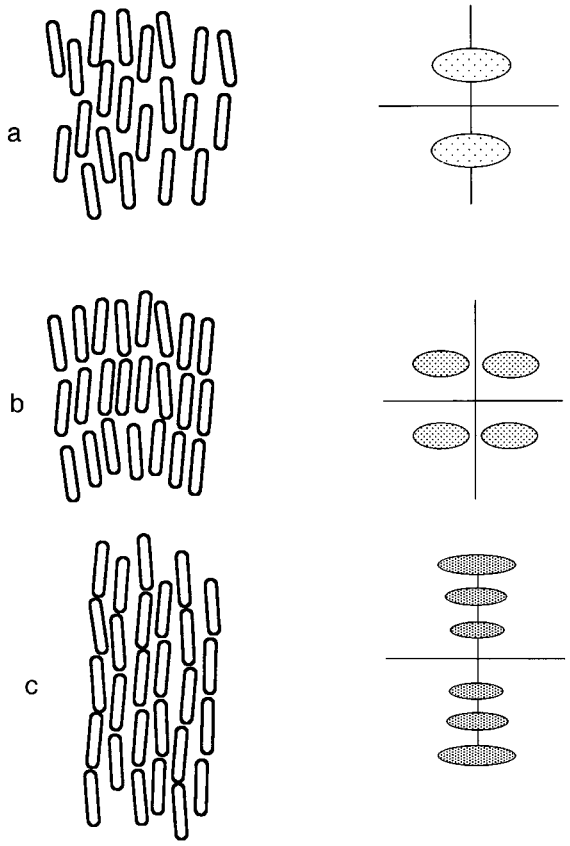

Figure 1. Possible molecular associations in the nematic phases (left) and corresponding X-ray patterns (right): (a) classical nematic phase with orientational ordering, (b) skewed cybotactic nematic phase, and (c) molecular strings.

are intermediate between low molar mass LCs and polymeric LCs.[7] They have a strong tendency to form

* Author to whom correspondence should be addressed.
† Western Michigan University.
‡ Science Application International Corp.
§ Cornell University.
|| Wright-Patterson Air Force Base.
⊗ Abstract published in *Advance ACS Abstracts,* November 1, 1996.

S0024-9297(96)00770-X CCC: $12.00

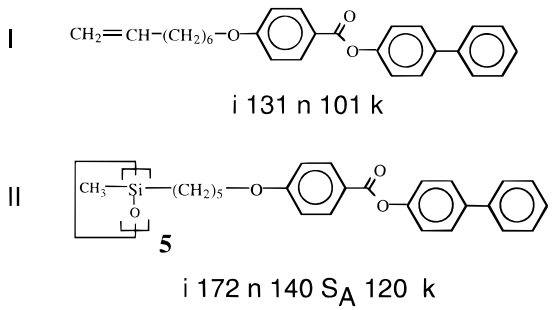

Figure 2. Chemical formulas of LC compounds **I** and **II** studied and schemes of phase transformations.

nematic and smectic phases at elevated temperatures which can be vitrified into a glassy state. Due to their low melt viscosity, good alignment can be obtained using electric, magentic, or shear fields. One particular compound in the nematic phase displayed strong diffuse low-angle meridional reflections with a complicated modulated intensity of the X-ray patterns.[8] To explain this observed X-ray behavior, string formation was proposed.[4] Since then, a systematic experimental investigation of cyclic LCs with other backbones with the same pendant mesogen was undertaken.[14] First attempts to simulate molecular associations of cyclic LCs indicate that a reasonable match to the experimental *d*-spacings can be obtained assuming an overlap of mesogenic groups within small clusters of limited sizes.[11,12] Similar but weaker low-angle X-ray scattering was observed for linear siloxane LC polymers several years ago (and in this recent work) which were explained by a modulation of electron density within areas of separately packed siloxane backbones and mesogenic side groups.[9,10] However, these speculations are not supported by a complete analysis of the X-ray scattering and no quantitative models of molecular arrangement have been proposed yet.

In the present paper, we focus on analyzing the molecular arrangement of these cyclic LC oligomers and, especially, on the relationships between the spatial arrangement of these molecules and scattering phenomena in the low-angle X-ray scattering region. Detailed results of molecular modeling for a cyclic LC compound are compared to modeling performed on the mesogenic unit itself. The goal of this study is to elucidate the reasons for the appearance of strong modulated X-ray low-angle reflections in cyclic LC oligomers and polymers as described in detail in the next paper[14] as well as to discuss simulation limitations of the quantitative models of molecular association in the nematic phase.

Experimental and Computational Approaches

Summary of Known Experimental Results. Chemical formulas of LC compounds discussed here are presented in Figure 2 along with the phase transformations determined earlier.[3,14] Detailed simulations discussed here were done for a single mesogenic group (compound **I**, a model of the monomeric unit) and for a cyclic LC (compound **II**) with five mesogenic groups attached to a central siloxane ring both shown in Figure 2. X-ray data for oriented LCs were obtained at the Cornell High Energy Synchrotron Source using a thermal cell with an applied electric field as described in detail elsewhere.[8] Experimental data shown in Figure 3 were obtained at 10 000 Hz with an applied field strength of approximately 1 V/μm. Up to six reflections with a modulated intensity distribution were observed for compound **II** in the nematic phase as shown in Figure 3b. These reflections persist into the smectic phase with the superposition of the Bragg layer reflection occurring (Figure 3c). This superposition is

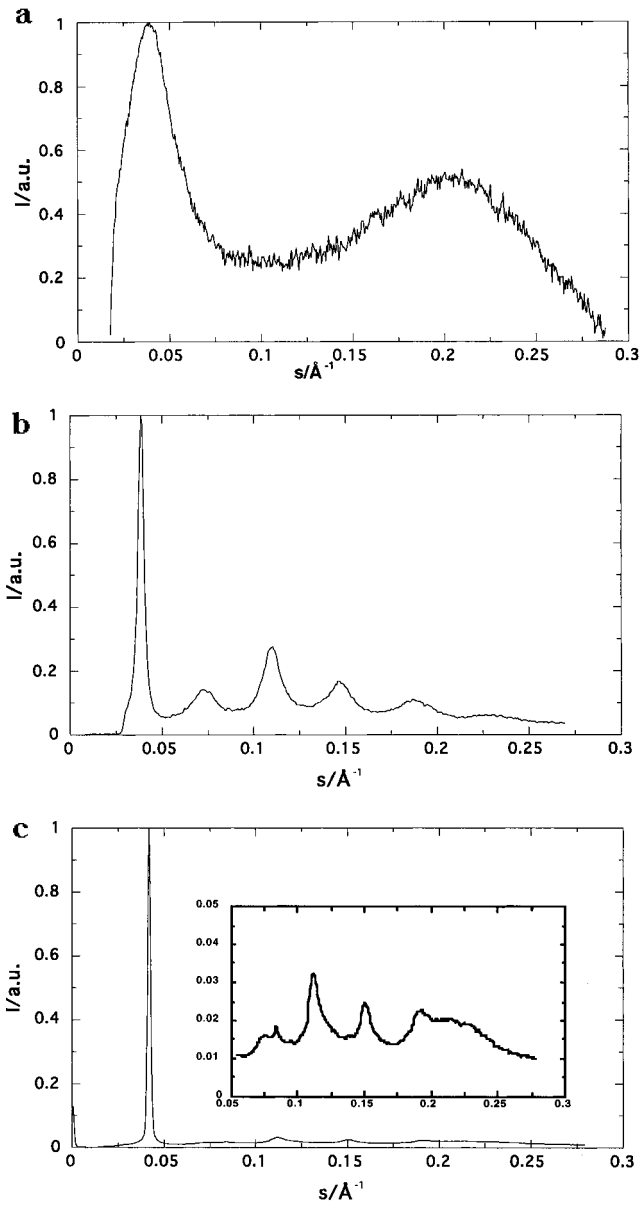

Figure 3. X-ray meridional scattering for nematic phases of compounds **I** (a) and **II** in nematic (b) and smectic (c) phases.

clearly evident in the second-order reflection, which shows the broad diffuse reflection underlying a sharp 002 peak (insertion in Figure 3c). Both of these meridional profiles can be contrasted to that of compound **I**, which shows a single broad diffuse reflection in the low-angle region (Figure 3a). Although not evident on the profile, several very weak additional reflections were present for compound **I** at higher angles as indicated in the table.

Computational Technique. Molecular modeling was performed on a Silicon Graphics Power Series workstation using the CERIUS[2] computer simulation package. The general procedures are similar to those described in the literature,[12,15,16] although some important features of our approach are subsequently discussed. We used energy minimization and molecular dynamics to build an isolated molecule with the lowest energy conformation. First, an initial molecular model was built. Second, several cycles of molecular dynamics and energy minimization were applied. The molecular dynamics procedure was step-by-step annealing which included at least five molecular dynamic cycles followed by an energy minimization cycle. The temperature was increased gradually from 300 to 450 K and then decreased back to 300 K. After this stage, global energy minimization with at least 1000 steps was performed on the model. Following this procedure, the molecule was packed into a crystal unit cell and crystal lattice minimization was employed for various types of molecular arrangement. We used orthorhombic primitive and centered

unit cells to pack the molecules, although other symmetries (up to trigonal) were attempted as well. Step-by-step minimization of the lattice energy was done by allowing different levels of freedom for molecular motion such as positional displacement and rotation of the molecules in different directions along with variations of the unit cell parameters. To assure dense molecular packing at the initial stage, external compression along the *a*- and *b*-axes (typically, in the range of 10−30 kbar) and tensile stress along the *c*-axis (main axis of molecules) were applied. This procedure was aimed to mimic the internal orientational molecular field in nematic phases. To avoid artificial "squeezing" of molecules due to the external pressure, we used a "relaxation stage" as the final procedure to reach an energy minimum while keeping the external pressure close to zero (0.1 kbar). Finally, we did not "fix" small irregularities in molecular fragments, keeping in mind that a certain level of disorder naturally exists in mesophases with short-range local ordering of molecules.

In addition to building molecular models, the CERIUS package provides a broad range of possibilities for simulation of various X-ray properties of molecular models.[17] Below, we summarize those important for further discussion and simulations of X-ray data. To calculate isotropic scattering, $I(s)$ ("powder diffraction"), where s is a wavevector defined as $s = 2 \sin \Theta/\lambda$ (Θ is the half-scattering angle and λ is the wavelength used), and the Debye formula was used in the form

$$I(s) = D_o \sum_i \sum_k \frac{f_i(s)\, f_k(s) \sin(2\pi s r_{ik})}{2\pi s r_{ik}} \qquad (1)$$

where r_{ik} are interatomic distances between i and k atoms and f_i is a structural factor (see below). The Debye−Waller factor, D_o, defined as

$$D_o \sim \exp(-16\pi^2\mu^2(\sin\Theta)^2/\lambda^2) \qquad (2)$$

is caused by random fluctuations of the atomic groups (so called distortions of a I kind including thermal vibrations with an amplitude μ) and vacancies. For simulation of two-dimensional scattering $I(s_r, s_j)$ ("fiber diffraction") the Fourier-Bessel transformation was employed as defined by

$$I(s_r,s_z) = \sum_n [\sum_j f_i\, J_n(2\pi s r_{ij}) \cos(2\pi(s_z z_j - n w_j))]^2 + \sum_n [\sum_j f_i\, J_n(2\pi s r_j) \sin(2\pi(s_z z_j - n w_j))]^2 \qquad (3)$$

where J_n is nth order Bessel function and r_j, z_j, and w_j are cylindrical polar coordinates of atom j. One-dimensional scattering along the main molecular axis $I(s_z)$ ("meridional scattering") was calculated using the Debye formula for projection of all intermolecular distances on the *c*-axis of the model as defined by

$$I(s_z) = [\sum_j f_i \cos(2\pi s_z z_j)]^2 + [\sum_j f_i \sin(2\pi s_z z_j)]^2 \qquad (4)$$

Pair correlation functions $G(r)$ and partial pair correlation functions of specific elements $G_{AB}(r)$ (such as Si−O, O−O) were employed to estimate the contribution of various atomic groups to the density distribution

$$G(r) = 4\pi r(\rho^2(r) - \rho_o{}^2) \qquad (5)$$

$$G_{AB}(r) = 4\pi r(\rho_{AB}{}^2(r) - \rho_{oAB}{}^2) \qquad (6)$$

where $\rho^2(r)$ is the self-convolution of the atomic density and $\rho_o{}^2$ is the mean value of $\rho^2(r)$; $\rho_{AB}{}^2(r)$ and $\rho_{oAB}{}^2$ are the same functions for A and B type atoms. Finally, a complete calculation of the X-ray diffraction pattern for perfect crystal lattice can be done according to

$$I(hkl) = [\sum f_n \cos(2\pi(hx_n + ky_n + lz_n))]^2 + [\sum f_n \sin(2\pi(hx_n + ky_n + lz_n))]^2 \qquad (7)$$

where hkl are Miller indices and x_n, y_n, and z_n are fractional coordinates of atom n.

Finite sizes of scattering regions, L_i, different levels of lattice distortions of d-spacings (interplanar distances) in various directions, $g_i = \Delta d_i/d_i$, orientational ordering of molecular fragments, P, and thermal fluctuations, D_o, all are included in the simulations. Orientational disordering of molecular fragments is simulated, including P in the eq 3 via Legendre polynoms. The Debye−Waller thermal factor D_o in the form of eq 2 can be included in all calculations. For example, for the current simulations the amplitude of the Debye−Waller factor was 0.05−0.2 nm, typical for thermal vibration in liquid phases.[18] L and g parameters are not included in direct simulations but can be added at the final stage as angular-dependent broadening of X-ray peaks according to known experimental relationships.[19] All these parameters are varied in a wide range to fit the simulated X-ray patterns to the experimental data (intensity and shape of reflections, crystal sizes, distortion levels, and unit cell parameters).

Remarks on Scattering Properties of LC Systems. Before we discuss the specific results of the current modeling of LC compounds, we have to summarize some basic approximations and limitations of simulation procedures when applied to LC systems. A key element of such limitations is the absence of a complete scattering theory providing a set of analytical expressions for the consistent description of partially ordered systems in real space that can be used for numerical solution and simulation of their scattering patterns in reciprocal space. From this standpoint, a brief discussion on the most developed description of disordered structures, the paracrystalline theory of Hosemann,[18−21] and the most sophisticated computer package for these kinds of structural simulations, CERIUS²,[17] is in order.

Let us assume that we have a basic structural element (such as an atom or molecules) arranged in real space at definite positions with a density distribution ρ_i within the a region of finite size determined by a shape factor, $T(r)$. The distribution of the scattered intensity in reciprocal space, $I(s)$, can be calculated according to a general diffraction equation for homogeneous paracrystalline lattice structures[20] given by

$$I(s) = N_o[|f_o|^2 - |D_o|^2|f_o|^2] + 1/v_o|D_o|^2|f_o|^2 Z(s)^\wedge |S(s)|^2 \qquad (8)$$

where $\wedge$ is the convolution integral, N_o is the number of molecules, v_o is the volume of the molecule, and the first term is a diffuse small-angle contribution caused by random thermal fluctuations in the number of atoms or molecules in the volume v_o. The term $|f_o|^2 = f(s)\, f^*(s)$ is the average molecular form-factor of the density distribution $\rho(r)$ in a structural element. $Z(s)$ is a factor of interatomic distances and $Z(r)$ represents lattice statistics. $Z(s)$ (also called the interference function) is the Fourier transform of the lattice statistics which is the frequency of an occurrence of the distances between two elements, i and k. $Z(r)$ is also called the pair distribution or correlation function, $G(\rho_{ik})$, when multiplied by the density distribution within a basic element $\rho(r_i)$. The shape factor, $S(s)$, is the Fourier transform of the lattice form-factor $T(r)$ in real space which limits the volume of the scattering region (domain) and defines the density distribution within a finite regions as $\rho(r) = \rho_\infty(_r)\ T(r)$ caused by finite sizes of ordered regions in a polydomain structure.

The intensity distribution $I(s)$ contains the complete information concerning the internal structure of matter including the density distribution in the basic structural elements (the coordinates of the atoms in molecules, for example), the level and anisotropy of thermal vibrations, the spatial arrangement of the molecules, the level of distortions, and the shape and size of ordered regions. However, such a complete analysis can be done only for an ideal single crystal. For partially ordered materials (such as LCs), where the complex shape of the pair distribution function is unknown, direct application of the general diffraction eq 8 is impossible. The paracrys-

talline theory, based on specific assumptions about edge statistics and independent fluctuations of the unit cell edges in three dimensions, provides approximate analytical solutions for $Z(r)$ and relationships for the analysis of partially ordered structures.[18,21−23] This theory has proven valid for the one-dimensional case and is useful for analysis of three-dimensional systems.[18−23]

This summary allows an analysis of the level of approximation used in the computer simulation package employed here. Computer programs for structural simulation are based on the "ideal crystal" version of the general diffraction eq 8 or direct summation of Fourier components (eq 7). Usually, simulation approaches treat analyzed structures as an infinite, ideal three-dimensional lattice with long-range positional ordering of the molecular motif. In such a case, the general diffraction relationship (8) is simplified to

$$I(s) \sim |D_o|^2 |f_o|^2 |S(s_{hkl})|^2 \tag{9}$$

Broadening of the diffraction peaks due to lattice distortions and limited sizes of scattering regions is incorporated in the final $I(s)$ according to known behavior. Another approach which is applicable to small molecular clusters and isolated molecules and considers the form-factor $F_{cl}(s)$ of a cluster as a whole calculates $I(s)$ by

$$I(s) \sim |D_o|^2 |F_{cl}|^2 \tag{10}$$

Both these approaches are used here for simulation of the X-ray properties of molecular models.

However, for LC systems with high degrees of positional distortions, the sizes of coherent scattering regions are determined by the characteristic damping radius of positional correlations (correlation length). In this case, the scattering function $I(s)$ is determined by the interference function $Z(s)$ related to the lattice statistics $Z(r)$ (or correlation function $G(r)$). Statistics of the interatomic distances (damping of correlations) determines the shape of $I(s)$. This approach requires knowledge of the nature of short-range ordering and interatomic correlations in simulated systems. Unfortunately, these capabilities are not found in modern computer simulation packages.

Simulations of X-ray scattering behavior according to eqs 9 and 10 are based on long-range positional ordering and do not thoroughly consider positional distortions of molecular ordering. These equations do not address the problem of a detailed description of short-range ordering with high levels of fluctuation typical for a LC state. The paracrystalline approach describing the lattice distortions as the accumulation of random fluctuations of a second kind by multiple convolution of partial distribution functions is not currently integrated with molecular modeling packages. Two different possibilities exist in our computer package to imitate short-range ordering in a simplified way. The assignment of extremely small crystal lattice sizes (not more that two to four d-spacings) with a very high value of the distortion factor g (up to 10%) is the first approach. These parameters are similar to those normally used for the description of short-range order within the paracrystalline theory or with the quasicrystalline approach.[18−21] The second possibility includes controlled displacements of selected structural units out of their exact positions in the crystal lattice (distortions of ideal positions).[17] This approach works if one needs to introduce a microscopic defect with known internal structure in an ideal crystal lattice (such as stacking faults), but this approach is not very adequate for describing short-range order caused by statistical random fluctuations. Obviously, these oversimplifications of local molecular correlations result in underestimation of the actual distortions in nematic phases. This results in systematic differences between simulated and experimental X-ray scattering.

General limitations of our molecular modeling techniques are also briefly mentioned. First, molecular models are minimized to built molecules with the lowest total energy. To assure this we use several different initial states and use molecular dynamics cycles followed by energy minimization. We believe that our models are reasonably close to the global minimum and possible deviations do not effect their scattering properties. However, we cannot exclude that some other possible conformations can be achieved.

Second, one can expect that for ideal molecular models in the crystalline state virtually all bonds in the alkyl spacers should be in a trans-conformation. However, this is not true for nematic and disordered smectic phases where a substantial fraction of the bonds adopt a gauche-conformation. In fact, in nematic polymeric LC phases about $^1/_5$−$^1/_4$ of atomic bonds in the spacer groups reside in a gauche-conformation with g^+tg^- type kink defects being very common.[24] The presence of these kink defects with two gauche-conformers per one kink causes shrinkage of the total length of spacers by 0.25 nm along the alkyl chain, as demonstrated by molecular modeling.[25] For 8−12 bonds in two spacers of oppositely oriented mesogenic groups in compound **II** (see Figure 3), one can expect the appearance of one to two kink defects. Thus, the total length of the molecules along the director in the nematic phase could be 0.25−0.5 nm shorter than for the minimum energy molecular model in a fully extended conformation. As a result of this difference, one can expect larger geometrical dimensions and, therefore, larger d-spacings for a simulated model with fragments in the extended conformation. Indeed, such overestimation of d-spacings in the c-direction was frequently observed in our simulations.

Third, various fragments of oligomeric and polymeric LCs usually possess very different local ordering. For example, flexible fragments of backbone and spacer groups are much more disordered as compared to locally ordered rigid mesogenic groups.[5,26] This statistical local disordering is not incorporated in our models. The absence of more disordered flexible fragments in our models results in the overestimation of the total positional ordering and underestimation of the rate of correlation decay. As a result of such underestimation, simulated X-ray peaks are much sharper than expected for given sizes of the molecular associations with short-range ordering. In addition, diffuse background scattering caused by thermal fluctuations[27] is not included in simulated X-ray patterns at all. These and other differences and consequences will be discussed in appropriate places.

Results and Discussion

"Monomeric Unit" (Compound I). Low-angle X-ray meridional scattering of monomeric compound **I** in the nematic phase (Figure 3) shows only one strong reflex at 2.6 nm and very weak broad additional reflections with d-spacings of about 1.2, 0.8, and 0.6 nm which are not seen in the meridional profile shown in Figure 3a. These reflections can be observed visually on an overexposed image, however. An example of a model for a single "monomer unit" is presented in Figure 4a, and all structural parameters are collected in the Table 1. Minimization of the total energy of the molecule packed in a crystal lattice led to the following parameters of the unit primitive orthorhombic cell I: a = 0.62 nm, b = 0.38 nm, c = 2.62 nm, and density of 1.08 g/cm^3. The main axis of the molecule is oriented along the c-edge. If we allow variation of the angle α of the unit cell, the new set of parameters are slightly different: a = 0.68, b = 0.38, c = 2.72, α = 65° with a density of 1.05 g/cm^3 (cell II as shown in Figure 4). The c-size of both unit cells is very close to the experimentally observed value of d-spacing in the meridional direction of 2.62 ± 0.1 nm. The lattice energies of both cells are also very close. However, the second "skewed" cell predicts a splitting of the low-angle X-ray reflex with a splitting angle φ = 25° that is close to the X-ray pattern observed experimentally. The simulated two-dimensional X-ray pattern for the unit cell II of compound **I** with lattice parameters shown above is presented in Figure 4b (for comparison with experimental results, see ref 14).

Table 1. Structural Parameters of LC Compounds in the Liquid Crystalline Phase[a]

	d_1, nm	d_2, nm	d_3, nm	D, nm	L_c, nm	g_c, %	P_2
			Compound **I**				
experiment	2.62	1.23	0.81	0.49	14	none	0.54
modeling	2.47−2.62	1.23−1.31	0.82−0.87	0.38−0.68	10−15	5	0.6
			Compound **II** (Nematic)				
experiment	2.58	1.38	0.91	0.53	28	4	0.7
modeling	2.7−3.0	1.44−1.59	0.9−0.97	0.5	25−30	−	0.6
			Compound **II** (Smectic Phase)				
experiment	2.38	13.1	0.90	0.46	49	none	0.67
modeling	2.78	1.39	0.92	0.4−0.7	40	1	0.6

[a] d_i is spacing for the first three low-angle X-ray reflections (c-direction of the unit cell or direction of the main axis of molecules); D is spacing of wide-angle reflex (a- and b-directions); L_c and g_c are size and distortion parameters of ordered associates along the c-direction, P_2 is orientational ordering parameter.

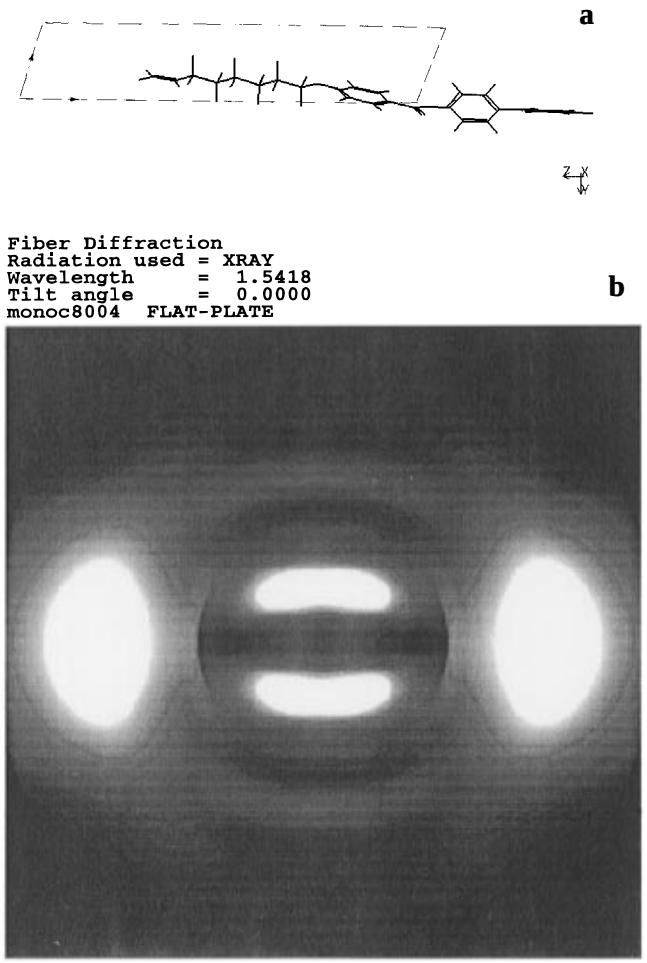

Figure 4. Molecular model of compound **I** packed in cell II (a) (the c-axis is horizontal) and a two-dimensional fiber X-ray diagram simulated for this unit cell (b) (the c-axis is vertical).

To fit simulated X-ray patterns with the experimental data (intensities of various orders of reflection, width, and azimuthal spreading of the low-angle reflection), we used a lattice factor with very small lattice sizes ($L_{a,b}$ = 2 −3 nm) and large distortion ($g = \Delta d/d$ = 10%) along the a- and b-axes. The limited sizes of ordered regions and very high level of lattice distortions required to simulate experimental data reflect short-range lateral ordering of liquid type typical for nematic phases.[28] For the structural parameters of the crystal lattice along the c-axis the best match can be obtained using L_c = 10−15 nm and g = 5−10%. These parameters indicate short-range longitudinal correlations in the nematic phase of compound **I**. Short-range ordering in the c-direction of the crystal lattice is expanded over four to five neighboring molecules. The optimal orientational parameter of molecules, P, used in these simulations is in the range of 0.6−0.7, which is close to experimental observations (Table 1). The size of the ordered regions along the c-axis obtained from molecular modeling (within 10−15 nm) covers the experimental value (14 nm) as well (see ref 14). Thus, for "monomeric" compound **I**, a model of the mesogenic group without the siloxane ring, the observed X-ray scattering phenomena can be easily explained by the formation of a distorted lattice with a primitive unit cell and short-range positional ordering of molecules along the all axes.

Cyclic LC (Compound II). A detailed analysis of X-ray properties was also completed for compound **II**, a five-membered ring with similar pendant mesogens as compound **I**. X-ray meridional scattering shows a very strong and relatively sharp peak at 2.6 nm and several additional, very diffuse, periodic weak halos of which the 0.9 nm reflection corresponds to the highest intensity (Figure 3b).[14] At a lower temperature, this compound displays a smectic phase with a slightly shorter d-spacing of 2.4 nm although the primary reflections peak intensity is an order of magnitude higher than in the nematic phase. In addition, a second-order smectic layer peak is observed superimposed on the the second diffuse reflection.

To test the spatial properties of these molecules in real space, pair correlation functions, $G(r)$, were calculated for the molecular models of a single molecule (Figure 5). Analysis of total pair correlation function, $G(r)$ (Figure 5a), shows a sharp peak at 0.15 nm corresponding to a standard set of the overlapped short interatomic distances for C−C, C−O, C═O, and Si−O bonds and second sharp peak at 0.25 nm for C−C−C, C−O−C, and similar distances. Additional broad and less intensive maxima at 0.5, 0.7, 0.9, 1.2, 1.7, (weak), and 2.3 nm (weak) correspond to sets of intramolecular and intergroup distances along and transverse to the main molecular axis. Apparently, this set of interatomic distances is significantly affected by strong partial contributions of intramolecular distances associated with "heavy" Si atoms concentrated in the ring. To estimate the significance of these contributions and their role in the statistics of interatomic distances, we calculated modified functions $G(r)$ for the same single molecule but with all Si atoms replaced with carbon atoms and partial correlation functions $G_{Si-O}(r)$ and $G_{O-O}(r)$ (Figure 5b−d).

As observed in Figure 5b, peaks on $G(r)$ below 0.8 nm remain almost unchanged after replacement of the Si atoms with lighter carbon atoms. On the other hand, the peak at 0.9 nm completely disappears and other maxima at $r > 1.3$ nm are almost completely smoothed out; the analysis of the partial correlation functions $G_{Si-O}(r)$ and $G_{O-O}(r)$ (Figure 5c,d) shows that Si−O and O−O distances significantly contribute to $G(r)$ peaks in

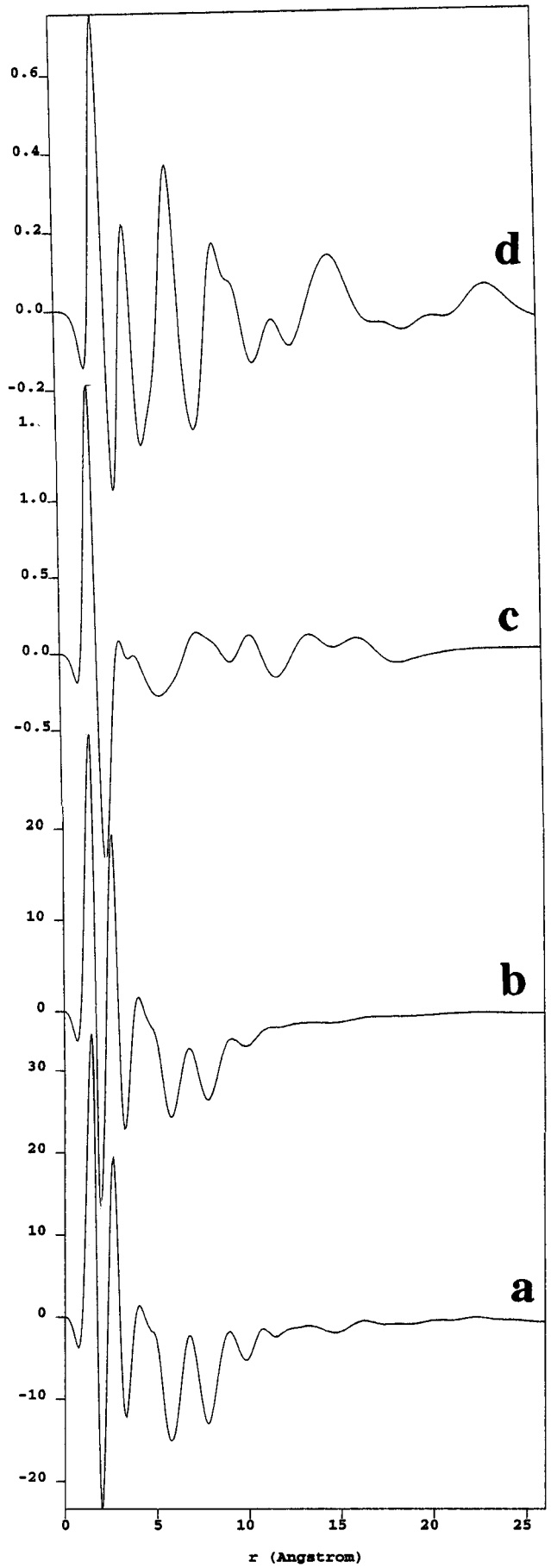

Figure 5. Pair correlation functions [$G(r)$] for molecular models of compound **II**: (a) $G(r)$ for compound **II**, (b) $G(r)$ for an analog of compound **II** with all Si atoms being replaced with carbon atoms, (c) $G_{Si-O}(r)$ for compound **II**, and (d) $G_{O-O}(r)$ for compound **II**.

the range of 0.6−1, 1.3−1.7, and 2.3 nm. These peaks are caused mainly by the distances between the siloxane rings and central parts (COO groups) of the attached mesogenic groups. Thus, the presence of heavy Si atoms emphasize these contributions in the total statistics of interatomic distances $G(r)$. The partial statistics of Si−O and O−O intramolecular distances [$G_{Si-O}(r)$ and $G_{O-O}(r)$] causes the presence of singularities on $G(r)$ and the form-factor (scattering function) of molecular associates, as will be discussed next.

Distribution of X-ray intensity along the meridional direction for an isolated molecule or a group of molecules is a form-factor of molecular association calculated by the Fourier transformation of electron density projected on the *c*-axis according to eq 4. To simulate the X-ray properties of possible associations of molecules in the nematic phase of compound **II**, we built a single row of aligned molecules (a "string"), as shown in Figure 6. The mutual arrangement and the number of molecules in the string are varied to reach the best fit to experimental data. Figure 6a shows an example of X-ray meridional scattering for a simple association of two molecules in a single string model. A gradual decrease of peak intensities versus scattering angle is observed for this model which contradicts experimental observations (Figure 3). Thus, a single string or head-to-tail packing of molecules in a row along the *c*-direction does not produce the modulation of meridional scattering observed experimentally for the nematic phase of cyclic compound **II**.

Only a more complicated association of the cyclic molecules with correlated arrangement of two rows of molecules shifted along the *c*-direction on a half of the molecular length ("double string") can produce a distribution of peak intensities close to the experimental observations for the nematic phase of compound **II** (for *d*-spacings see Table 1). An example of such association of two cyclic molecules and resulting X-ray meridional scattering are presented in Figure 6b. The intensities of the peaks on the X-ray curve are modulated with the first peak being the most intensive and the third peak with *d*-spacing about 0.9 nm having high intensity. The actual intensity of the first peak at 2.7−3.0 nm on simulated curves cannot be estimated unambiguously because of its proximity to zero scattering (scattering at small angles caused by the shape of molecules as a whole[20]). The cylindrical approximation used in the program can result in partial suppression of scattering in the "small-angle" region. For our model the first peak has intensity 50−100% higher than the intensity of the third peak, which is slightly lower than that observed experimentally.

Two other features of the simulated X-ray curves reflect differences between short-range ordering of actual LCs and our molecular model. First, although the width of reflections fit nicely to the experimental ones, peaks themselves are much sharper than on the experimental curves (Figures 3 and 6). This is caused by different profile shapes: almost pure sinusoidal peaks for the computer model and Lorentz shape profiles typical for LC systems.[29−31] Lorentz profiles of experimental reflections have much wider wings caused by fast damping of positional correlations described by Debye correlation function for many mesomorphic polymeric systems[6] given by

$$G(r) \sim \exp(-x/\xi) \cos(2\pi s d) \qquad (11)$$

where ξ is a correlation length. As a result, experimental X-ray reflections for partially ordered systems with

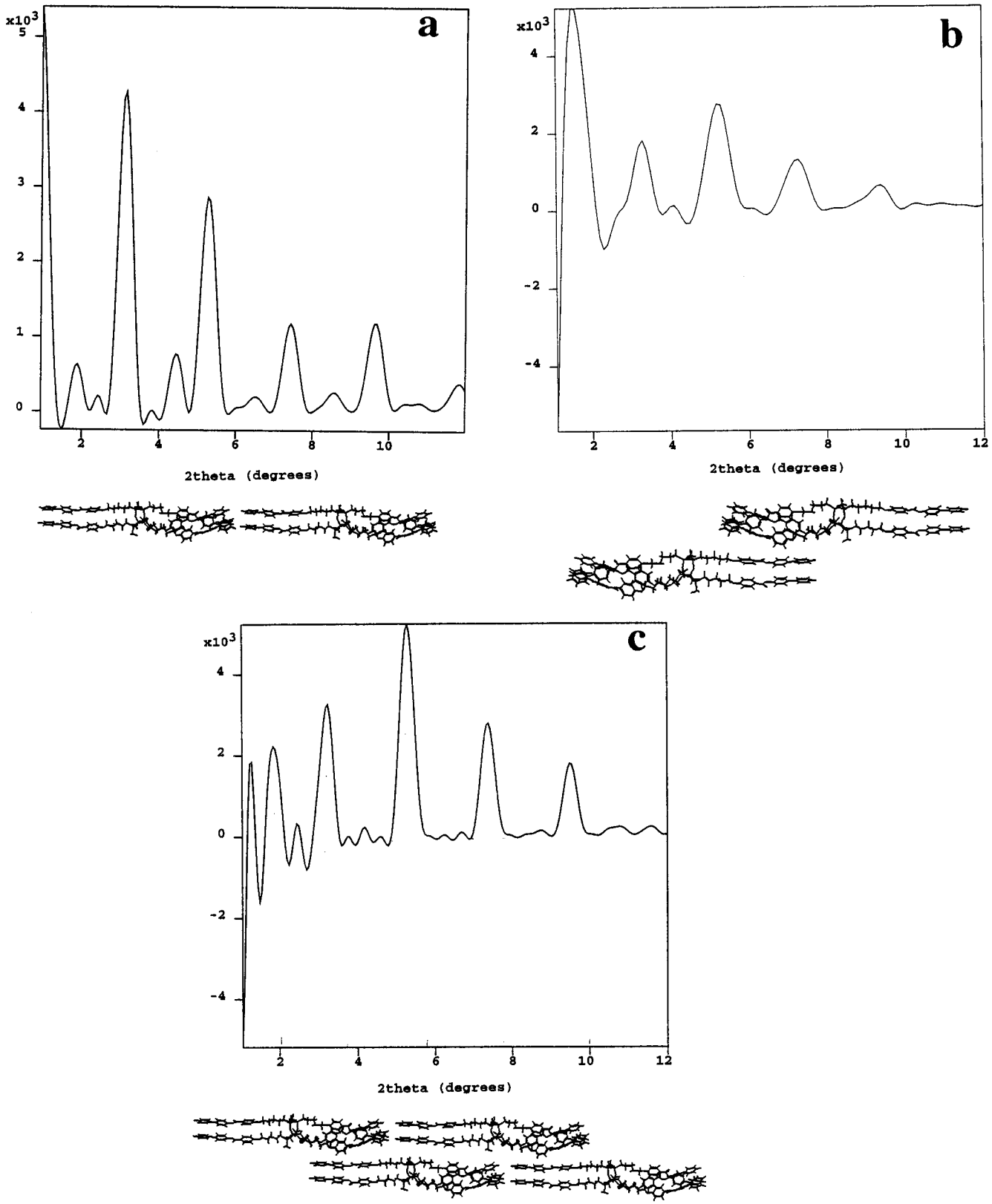

Figure 6. Meridional scattering simulated for a single-string model of the nematic phase of compound **II** (a), skewed association of two molecules (b), and the double-string model from four molecules total (c) of model compound **II**.

short-range ordering are much more diffuse than simulated ones. Partial overlap of the peak wings of the neighboring reflections creates a strong diffuse background (Figure 3). The absence of spatial decay of positional ordering in our model is a key reason for overestimation of the reflex sharpness and underestimation of the diffuse scattering background. Second, our computer modeling completely ignores complicated small-angle contributions caused by thermal fluctuations of the number of atoms in a given volume. This contribution is determined by the compressibility of the matter and thus is high in liquid and gases and low in solids.[27] This contribution is a rising function of a scattering angle, and its overlap with a scattering contribution caused by local inhomogeneities may result in a broad diffuse halo expanded over the total low-angle range. This phenomena is frequently observed for partially ordered LC and polymer systems.[6,18,27]

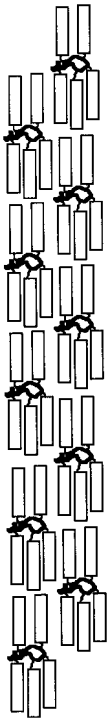

Figure 7. Sketch of molecular packing for double-string association from 10 cyclic molecules total of compound **II**.

Increasing the number of molecules associated in "double strings" results, as expected, in sharper X-ray peaks. This is demonstrated for the association of four molecules in Figure 6c. The number of molecules tested for the double-string models was in the range of two to eight. Comparison of our simulations with experimental data (see ref 14 for detailed analysis) allows an estimate of the number of molecules in the double string to be in the range of 10−12 for compound **II** in the nematic phase. This means that there are up to five to six cyclic molecules packed in the row in the *c*-direction with another row of five to six molecules packed side-by-side and shifted on a half-molecule (see a sketch of molecular packing for 10 molecules total in the double string in Figure 7).

We can speculate that this type of association may be caused by the specific shape of cyclic molecules with two and three mesogenic groups on different sides of the central ring (Figures 3 and 7). For this arrangement, a density deficit on one side of the central ring and steric limitations on the dense packing of molecules favor alternating packing of molecules. The simplest way to fullfill this requirement is the association of neighboring rows which results in the highest density of molecular packing with five mesogenic groups per "period" (Figure 7). An additional factor can be strong dipole−dipole interaction between mesogenic groups that promotes antiparallel packing of these groups belonging to neighbor molecules.[1]

Analysis of two-dimensional X-ray scattering from this double-string model shows that it reproduces not only the intensity modulation along the meridian but also the roof-like shape of reflections elongated along the layer plane observed for the oriented nematic phase of compound **II** (Figure 8a).[14] Distortion of the orientational order of molecules was simulated by using an orientational parameter, *P*, in the range 0.6−0.7 that corresponds to local deviations of molecular axes within ±30°. The resulting "real" X-ray pattern closely matches the experimental fiber diagram (see ref 14 for experimental data) and simulated orientational parameter is

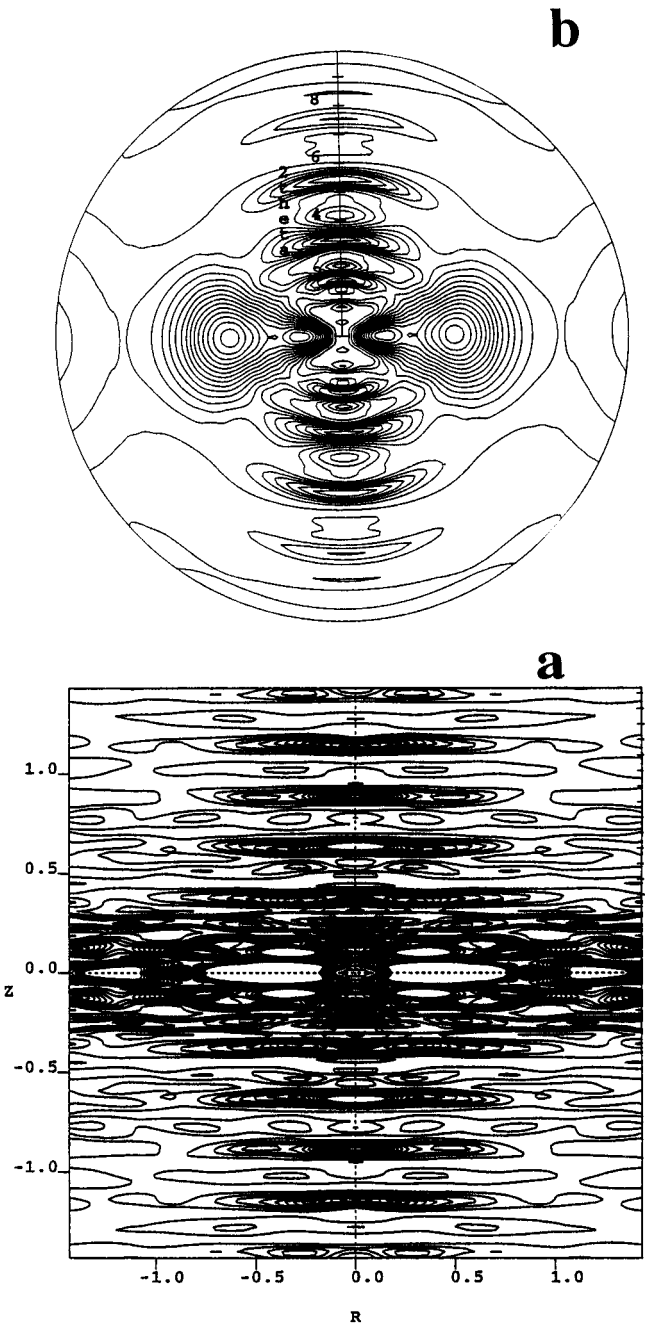

Figure 8. Two-dimensional X-ray diagram simulated for the double-string model of compound **II** with ideal orientational ordering (a) and with the level of disorientation $P_2 = 0.6$ (b).

close to the experimental value (Figure 8b, Table 1).

To clarify the influence of the high concentration of the Si atoms in the central ring on the resulting X-ray properties of cyclic LC molecules, we compare the meridional scattering for a double-string model composed of cyclic molecules with a central Si−O ring (total atomic weight of the group is 44), C−O ring (total atomic weight of the C−O group is 28), and C−C ring (total atomic weight of C−C group is 24) and with the ring completely removed (Figure 9). The meridional scattering with modulated intensity observed for the Si−O central ring compound is preserved for the compound with the Si atoms replaced by carbon atoms, although the intensity of peaks decreases significantly (about 50%) (Figure 9a,b). Replacement of all oxygen atoms in the ring with lower scattering power carbon atoms results in a further reduction (20%) of modulated meridional peaks (Figure 9c). The intensity of the first

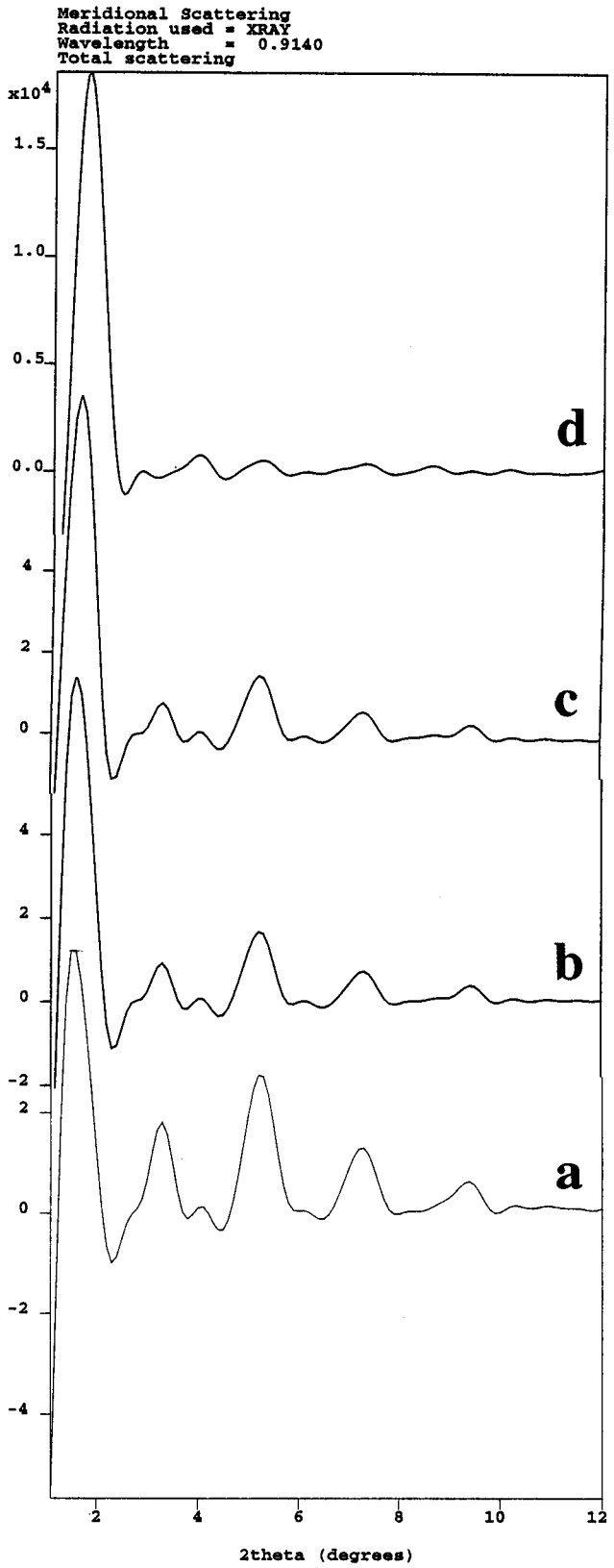

Figure 9. Meridional scattering simulated for the double-string model from four molecules of compound **II** (a), compound **II** with Si atoms replaced with carbon atoms (b), compound **II** with Si and O atoms replaced with carbon atoms, and compound **II** with removed central ring (d).

peak remains almost unchanged. Finally, removing the central ring results in complete disappearance of characteristic reflections: only the strong first peak and weak modulations of background scattering are observed (Figure 9d). Thus, we can conclude that the presence of the cyclic ring with high local concentration

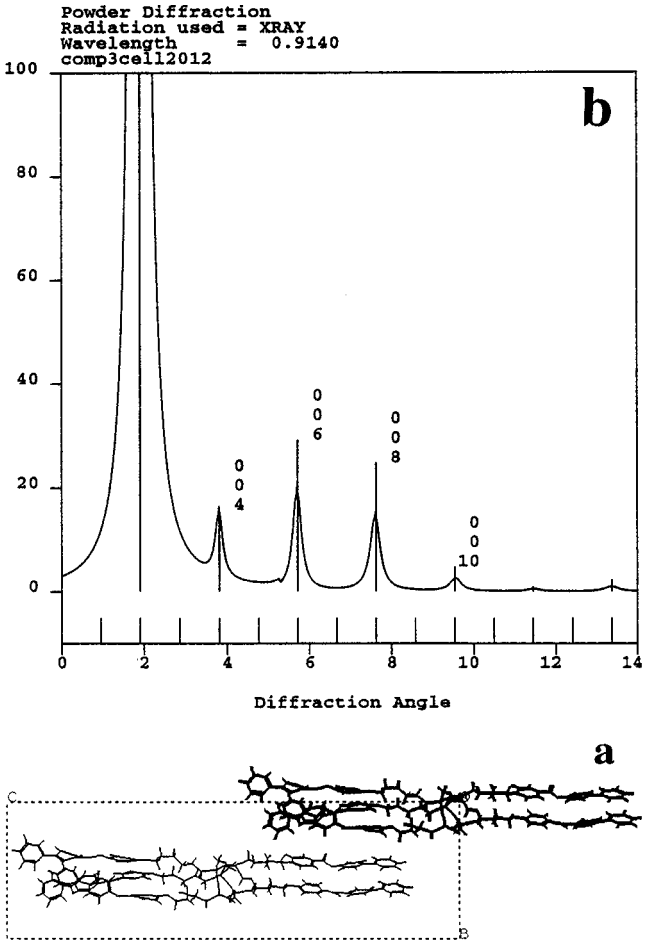

Figure 10. Molecular model of compound **II** in the smectic phase packed in the orthorhombic unit cell (a) and "powder" X-ray diagram simulated for this unit cell (b).

of Si−O atomic groups with strong scattering power is critical for the appearance of these low-angle periodic diffuse X-ray reflections with significant intensity. Weaker low-angle X-ray scattering phenomena for siloxane LC polymers[5,15] are probably the result of the intensity of X-ray reflections being smeared due to the spreading of flexible siloxane fragments. Cycling of the siloxane groups into more compact rings hinders rotation and restricts mobility of the Si−O units relative to a linear chain resulting in a high localization of strong scattering groups. This localization of the specific density distribution promotes the high intensity of these low-angle X-ray reflections. However, we have to point out that for siloxane linear LC polymer with identical mesogenic groups, the intensity of the periodic low-angle reflections is fairly strong (see experimental data for LC polymer with identical mesogenic groups in ref 14). For this case, an additional factor that must be considered is the presence of the long mesogenic groups which stabilize the local longitudinal ordering and, therefore, localization of the siloxane fragments.

To explore an alternative approach to simulate the X-ray data, we used the lattice approximation (long-range ordered crystal lattice) given by eqs 7 and 9. The cyclic molecules were packed into a distorted lattice and the lattice energy was minimized (similar to the procedure employed for compound **I**; see above). The results of the best fit was a body-centered orthorhombic unit cell with parameters $a = 0.67$ nm, $b = 1.8$ nm, and $c = 5.56$ nm and a density of 1.04 g/cm^3 (Table 1). This type of molecular packing and X-ray isotropic scattering for this model of packing are presented in Figure 10. The

cyclic molecules packed into the body-centered orthorhombic unit cell causes the appearance of even [(002), (004), (006), and (008)] orders of reflection along the *c*-axis with periodicities fairly close to those observed experimentally (Table 1). *d*-Spacings for molecular models are usually 0.1−0.3 nm larger than the experimental values due to the extended conformation of our computer models, as discussed above. In addition, modulation of the intensities of high order of reflection is close to that experimentally observed. However, the intensity of the (002) order is an order of magnitude higher than the other reflections and the (006) reflex constitutes only a small fraction of the total intensity (Figure 10). This contradicts the experimental observations for compound **II** in the nematic phase (Figure 3).[14] Attempts to "improve" the fit by introducing additional distortions along the *c*-axis made this discrepancy worse. Therefore, the "lattice" approach does not represent molecular packing in the nematic state because of an overemphasis of positional ordering in computer models of a perfect crystal lattice.

However, this lattice model does fit the experimental X-ray data for compound **II** in the smectic phase (Figure 3c) nicely. The ratio of the intensities of the first order and other reflections, modulation of intensities, and *d*-spacings all are close to experimental observations (Table 1). The best fit can be obtained for a lattice size of 40 nm and a distortion factor of $g = 1\%$ in the *c*-direction that is close to the parameters deduced directly from experimental data (Table 1).[14] That corresponds to the expansion of positional correlations over 14 molecules in the *c*-direction which is a lower limit expected for polymeric smectic phases.[6,30,31] Local molecular arrangement for this model is very similar to the double-string association proposed for nematic phase (compare Figures 6 and 10). It is also interesting to note the presence of the sharp Bragg reflexes overlapped with the second diffuse periodic reflection slightly out of register with the Bragg periodicity from the one-dimensional smectic lattice (see insertion in Figure 3c). This phenomena indicates significant contributions of both factors in total scattering: sharp peaks arising from the interference function of a one-dimensional layer lattice [$Z(s)$ in eq 8] and more diffuse contributions arising from the molecular form-factor [$f_o(s)$ in eq 8]. Our molecular modeling cannot provide further insight on this issue, but our results underline a very close similarity of the local molecular association in the double strings in the nematic phase and the layer ordering of cyclic molecules in the low-temperature smectic phase.

Conclusions

The analysis of computer simulations of X-ray properties of oligomeric LC compounds with mesogenic groups attached to the siloxane central ring shows that the presence of strong low-angle X-ray reflections in nematic phases is caused by local association of the molecules. The cyclic molecules form double-string associations with up to six molecules packed in a single string (or up to 12 molecules total). This type of association can be related to the specific shape of cyclic molecules with two and three mesogenic groups on different sides of the central ring that favors alternating packing of molecules because of a density deficit on one side of central ring and steric limitations on the dense packing of molecules.

The presence of the cyclic ring with high local concentration of Si−O atomic groups with strong scattering power turned out to be critical for appearance of low-angle X-ray reflections with significant intensity. Cycling of siloxane groups into short rings hinders rotation, restricts the mobility of entangled "backbones", and results in a high localization of high scattering Si−O groups. This phenomena enhances the specific density distribution caused by singularities of correlation functions because of strong contributions of Si−O and O−O interatomic distances (ring-mesogenic groups) and promotes high intensity of low-angle X-ray reflections. The intensity of similar X-ray reflections observed for conventional siloxane LC polymers is smeared because of spreading of unrestricted flexible siloxane fragments.

Finally, we can conclude that computer simulation of X-ray properties of partially ordered systems should be carried out with caution. The programs use the "lattice approximation" that is valid and works quite well for perfect crystal lattices and highly ordered mesophases like smectics. However, this approach underestimates local distortions of positional ordering and cannot describe adequately short-range molecular ordering of nematic phases. Application of straightforward calculations of form-factor of molecular clusters can reproduce major features of X-ray scattering patterns but falls short of describing many fine details such as diffuse background scattering, peak profiles, and exact *d*-spacings. The development of new computer simulation procedures based on the diffraction theories of disordered systems is required for further progress.

Acknowledgment. This work is supported by AFOSR, Contract F49620-93-C-0063, and was initiated during a summer visit of V.V.T. to Wright Laboratory supported by Summer Faculty Research Program, AFOSR. The authors thank Dr. S. S. Patnaik for helpful discussions and assistance. T.J.B. acknowledges Air Force Contract F33615-95-C-5423.

References and Notes

(1) De Gennes, P. *Physics of Liquid Crystals*; Claredon Press, New York, 1974.
(2) De Vries, A. *Mol. Cryst. Liq. Cryst.* **1981,** *63*, 215.
(3) Gresham, K. D.; McHugh, C. M.; Bunning, T.; Grane, R. L.; Klei, H. E.; Samulski, E. T. *J. Polym. Sci. Chem.* **1994**, *A32*, 2039.
(4) McNamee, S. G.; Bunning, T.; Patnaik, S. S.; McHugh, C. M.; Ober, C. K.; Adams, W. W. *Liq. Cryst.* **1995**, *18*, 787.
(5) Davidson, P.; Levelut, A. M. *Liq. Cryst.*, **1992**, *11*, 469; Deniz, K. U.; Pepy, G.; Kelbi, P.; Farnoux, B.; Parette, G. *Mol. Cryst. Liq. Cryst.* **1985,** *127*, 81; Wedler, W.; Hartmann, P.; Bakowsky, U.; Diele, S.; Demus, D. *J. Mat. Chem.* **1992**, *2*, 1195.
(6) Tsukruk, V. V.; Shilov, V. V. *Structure of Polymeric Liquid Crystals*; Naukova Dumka: Kiev, 1990.
(7) Bunning, T.; Kreuzer, F.-H. *Trends Polym. Sci.* **1995**, *3*, 318.
(8) McNamee, S. G.; Bunning, T.; McHugh, C. M.; Ober, C. K.; Adams, W. W. *Liq. Cryst.* **1994**, *17*, 179.
(9) Hotz, W.; Strobl, G. *Coll. Polym. Sci.* **1989**, *267*, 889.
(10) Muegge, J.; Zugenmaier, P. *Mol. Cryst. Liq. Cryst.* **1988**, *113*, 193.
(11) Socci, E. P.; Farmer, B. L.; Bunning, T. J.; Pachter, R.; Adams, W. W. *Liq. Cryst.* **1993**, *13*, 811.
(12) Pachter, R.; Bunning, T. J.; Adams, W. W.; Socci, E. P.; Farmer, B. L. *Makromol. Chem. Theory Simul.* **1993**, *2*, 337.
(13) Lipatov, Yu. S.; Tsukruk, V. V.; Shilov, V. V.; Kostromin, S.; Shibaev, V. P. *Polym. Sci. USSR* **1987**, *B29*, 411.
(14) Bunning, T.; Korner, H.; Tsukruk, V. V.; McHugh, C. M.; Ober, C. K.; Adams, W. W. *Macromolecules* **1996**, *29*, 8717 (following article in this issue).
(15) Roe, R. J. *Computer Simulation of Polymers*; Prentice-Hall: New York, 1991.
(16) Tsukruk, V. V. *Polymer* **1992**, *33*, 2605.
(17) CERIUS^2, Molecular Simulations, version 3.2, 1994.
(18) Lipatov, Yu. S.; Shilov, V. V.; Gomza, Yu. P. *X-ray Analysis of Polymer Systems*; Naukova Dumka: Kiev, 1982.
(19) Gunier, A. *X-ray diffraction in Crystals, Imperfect Crystals, and Amorphous Bodies*; Dover Publishers: Davis, CA, 1994.

(20) Hosemann, R.; Bagchi S. N. *Direct Analysis of Diffraction by Matter*; North Holland Publ. Co.: Amsterdam, 1962.
(21) Vainstein, B. K. *Diffraction by Chain Molecules*; Nauka: Moscow, 1964.
(22) Hosemann, R. *J. Polym. Sci.* **1967**, *C20*, 1.
(23) Hosemann, R. *Coll. Polym. Sci.* **1982**, *260*, 864.
(24) Plate, N. A.; Gordon, M., Eds. *Advances in Polymer Science* Springer-Verlag: Berlin, 1984; Vols. 59−61.
(25) Pechhold, W. R.; Grossmann, H. P. *Faraday Disc. Chem. Soc.* **1979**, *68*, 58.
(26) Tsukruk, V. V.; Shilov, V. V.; Lipatov, Yu. S. *Macromolecules* **1986**, *19*, 1308.
(27) Kratky, O.; Glatter, O., Eds. *Small-angle X-ray Scattering*; Academic Press: New York, 1982.
(28) Luckhurst, G.; Gray, G. W., Eds. *The Molecular Physics of Liquid Crystals*; Academic Press: New York, 1979.
(29) Tsukruk, V. V.; Shilov, V. V.; Lokhonya, O. A.; Lipatov, Yu. S. *Sov. Phys. Crystallogr.* **1987**, *32*, 88.
(30) Tsukruk, V. V.; Shilov, V. V. *Polymer* **1990**, *31*, 1793.
(31) Tsukruk, V. V. *Makromol. Chem., Symp.* **1991**, *44*, 109.

MA960770O